UNIVERITY OF TEHRAN

COMPUTATIONAL MODEL OF L6 LAYER, CORTICAL GRID CELLS

SIMULATION OF SPIKING CORTICAL GRID CELLS USING LOCATION INPUT OF MOVEMENT

AUTHOR

ARASH NIKZAD

Student No. 610301195

SUPERVISOR

MOHAMMAD GANJTABESH

TEHRAN, JULY 2024

Contents

1 Introduction

In recent years several types of neurons were discovered in the hippocampal region, notably in the entorhinal cortex, that encode allocentric spatial information. Among those newly discovered types of neurons are so-called grid cells. These neurons exhibit a peculiar kind of firing pattern. Every grid cell covers the entire environment of the animal with a virtual, triangular lattice and whenever the animal passes through a vertex of this lattice, the grid cell fires. New discoveries by Jeff Hawkins and his team at Numenta suggest the existence of cortical grid cells in the neocortex as an essential component of our brain in the ***Thousand Brains Theory of Intelligence*** based on cortical columnar structure of our brain.

In this project we are trying to implement a cortical grid-cell using the existing computational models as **L6** layer in a cortical column and simulating a circut of always on cortical column redundent to noise.

2

Rat Movement Simulation

To understand grid cell activity in the neocortex, we must simulate movement through space, as these cells are crucial for spatial navigation and memory. In "Rat Movement Simulation," we create a model of a rat's movement within a defined area to observe grid cell behavior.
This simulation generates input data for our computational model, replicating how grid cells encode positional information. With this foundation, we can build and run simulations on our grid cell model, revealing the principles of their dynamics and role in spatial cognition.

2.1 Simulation

Here we simulate an simple movement of a rat (considered a single point in the plane), here we used 50×50 plane to simulate the area of movement which its size is not highly relevant to the activity of grid cells. The movement is simulated inside a circle of length $R = 10$ around the center locating at $(0, 0)$ and it's simulating the period of $6000ms$.

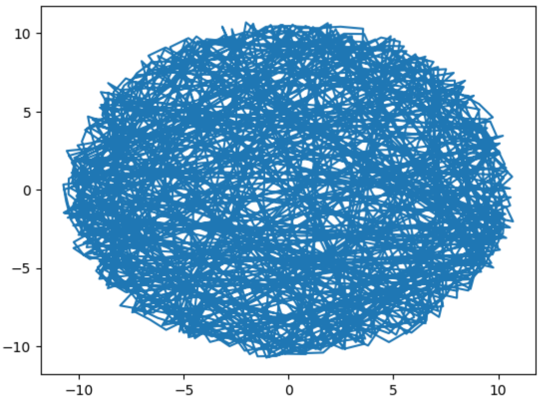

Figure 2.1: *the random path created by the simulation*

Figure 2.1 shows the general simulation for $6000ms$ and the intensity is to make sure that the random movement is not biased to specific locations or direction. however in order to make the movement of the rat more realistic we decreased the step size of the rat.

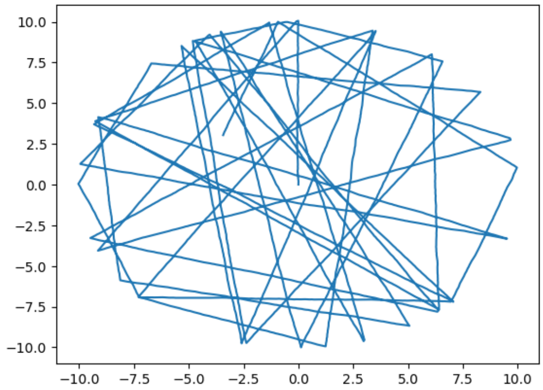

Figure 2.2: *smaller step size in order to have a more realistic movement in only 6 seconds*

Also the real movement might not be as straightforward and smooth as shown above, so we have added different amount of noisy movement to check the network stability later in this report.

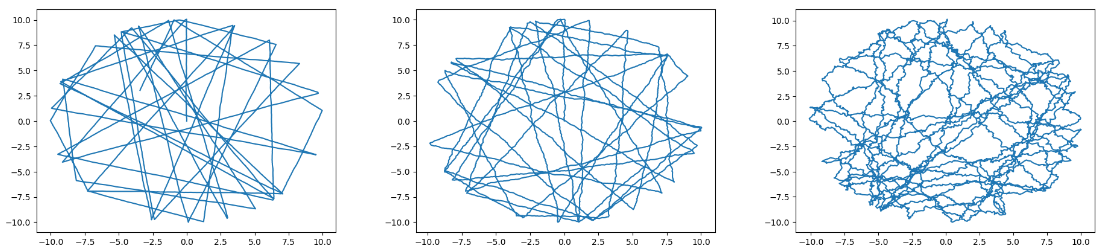

(a) `nosie-level = 0.2` **(b)** `nosie-level = 0.5` **(c)** `nosie-level = 1.2`

Figure 2.3: *different levels of noise in the simulation of rat's movement*

As we can see in Figure 2.3, the simulation has different levels of movement noise, in further experiments we expect the model to perform and be able to have a stable structure regardless of the noise.

in the next chater we introduce the spiking model of grid cells and analyse their behavior based on their location input we have created in this chapter.

3

Grid Cell Computational Model

In Chapter 3, we propose a spiking model based on the **Leaky Integrate-and-Fire (LIF)** framework and a **continuous-attractor-network (CAN)** model. This chapter focuses on analyzing the behavior of our model, aiming to replicate the distinctive activity patterns of grid cells and understand their role in spatial navigation. Through this analysis, we seek to gain deeper insights into the dynamics of grid cells within the neocortex.

3.1 Proposed Model

In recent years a number of computational models were proposed that offer several different mechanisms for the formation of grid-like firing fields and other properties of grid cells. The existing models of grid cells can be divided into three groups :

- **oscillatory-interference models**
- **continuous-attractor-network models**
- **self-organizing models**

Here we propose a spiking model using the idea of **continuous-attractor-network (CAN) models**. The network is 2D consisting of $N = 64 \times 64$ neurons throughout this simulation and assining a location of each between $(-\frac{n}{2}, +\frac{n}{2})$ where $n = 64$.

3.1.1 Neuron Dynamics

The spiking neuron model is the simple **LIF** model which here we use a **fast-spike** variation by having a very low threshold and high internal resistance.

Grid Cell Dynamics

$$\tau \frac{du}{dt} = -(u - u_{rest}) + R.I(t) \tag{3.1}$$

$$if\ u(t) = \theta \rightarrow Fire\ Spike + Reset\ (u = u_{rest}) \tag{3.2}$$

Aside from the basic dynamics of each neuron, they also have a **preferred direction**. In the real-life grid cell neurons found in the Medial Entorhinal Cortex (MEC) of a rat, these preferred direction are in an specterum of $[0, 2\pi]$ however in modeling we use only four main direction (*North, East, South, West*) for each neuron by assigning them the relative direction vector e_{θ_i}. The distribution of these directions along side the network is according to the following.

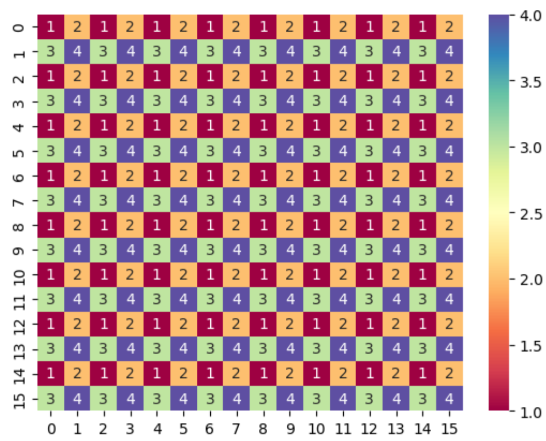

Figure 3.1: *The distribution of preferred direction of neurons in the grid cell module where each number represents a specific direction of (N, E, S, W)*

As we can see in Figure 3.1 The distribution is fairly uniform as we can see all four direction in every 2×2 subgrid of the grid cell module. In our simulation the following parameters are used.

Table 3.1: *LIF model parameters used throughout this project*

R	tau τ	threshold θ	v-rest	v-reset
10	5	-63	-65	-67

3.1.2 Synapses & Connections

The idea behind CANs is implemented using the specific connections the make along themselves. All connections are inhibitory and are some sort of **lateral-inhibtion** where each neuron inhibits a ring around themselves.

Lateal inhibtion Weights

$$W_{ij} = W_0(x_i - x_j - le_{\theta_i}) \tag{3.3}$$

Were x_i and x_j are the vectors of locations of corresponding neurons in the grid cell module, l is the direction scaler and e_{θ_i} is the unit direction vector of pre-synaptice neuron. Also $W_0()$ is a function constructing the ring as follows.

$$W_0(x) = ae^{-\gamma|x|^2} - e^{-\beta|x|^2} \tag{3.4}$$

In order for better understanding of the following weights we demostrate their behavior for each direction.

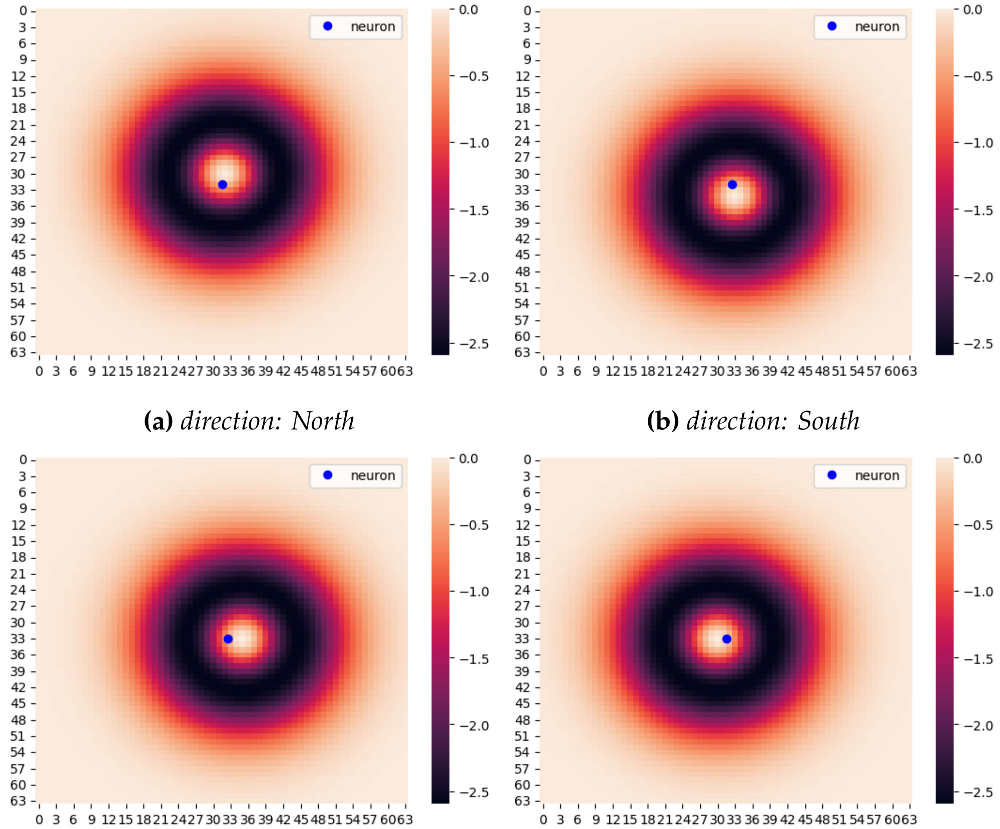

(a) *direction: North* **(b)** *direction: South*

(c) *direction: East* **(d)** *direction: West*

Figure 3.2: *Lateral inhibtion weights of neurons of each preferred direction*

Figure 3.2 gives us a better understanding of the preferred direction of each neuron and their influence on the lateral inhibtion of each neuron, giving them bias in the opposite of their preferred directions, giving more chance to neurons in preferred direction to activate and spike. different sets of parameters can shape rings of different strength and different sizes which will help us make different orientation and sizes of grid cells modules.

3.1.3 Input Encoding

In this stage the feedback (apical) connection between L6 grid cells and the L5 place cells are not taken into acount so the only input is the feedforward input of each neuron which has a baseline constant current and a voltage-based input current.

Feedforward input current

$$I_j = A(x_j)(I_{ext} + I_{vel} e_{\theta_i}.\vec{v}) \tag{3.5}$$

Here I_{ext} is the constant baseline input current, I_{vel} is the scaler of velocity-based input current and $\vec{v}$ is the speed vector in that iteration. Finally $A(x_j)$ is the envelope function used to handle the corner inhibitions of the grid cell modules as follows.

$$A(x) = e^{-\frac{|x|^2}{n}} \tag{3.6}$$

Where n is the number of rows and columns in the grid cell module.

3.2 Activity Pattern

Here we start to use the movement input we created in Chapter 2 and try to run the network and see the evolution of the network throughout time.

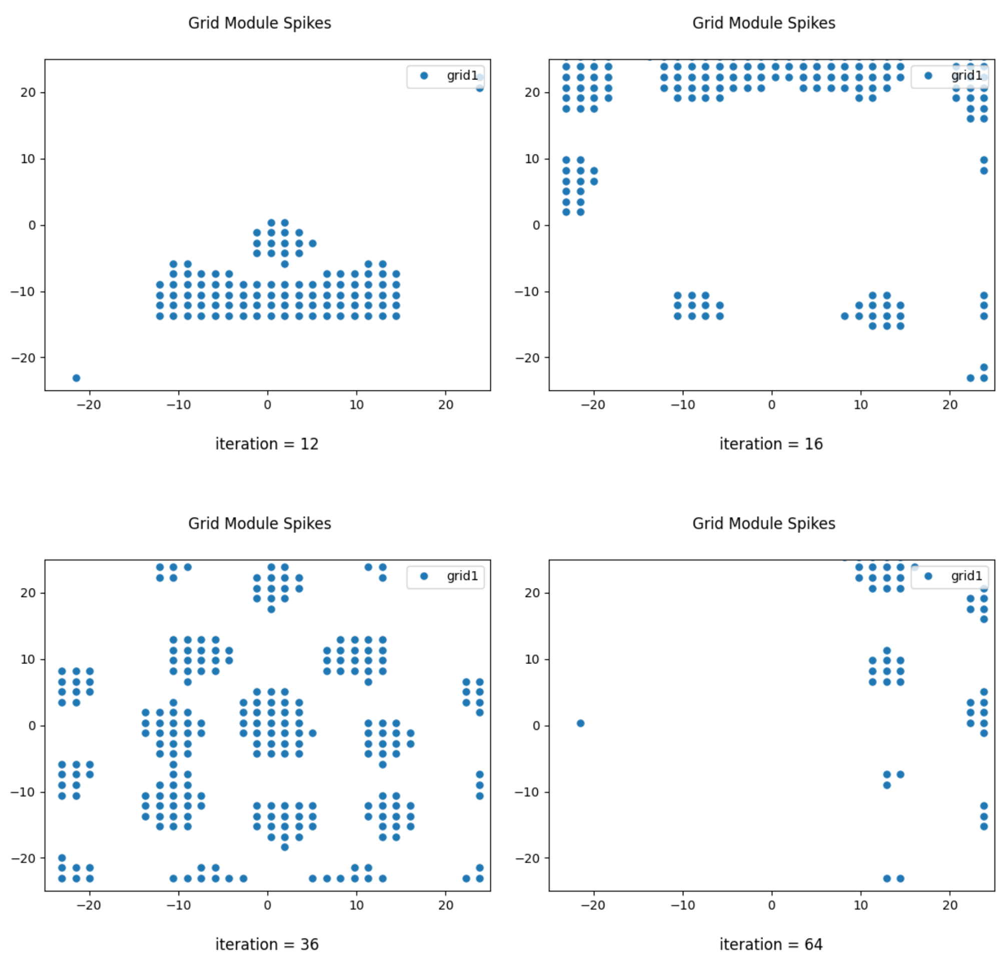

Figure 3.3: *different initial stages of the grid cell module before creating the hexagonal activity pattern*

As we can see in Figure 3.3, due to the envelope function network starts with random firings at the center, and its connection inhibits central neurons from firing a spike and the cornered neurons start to activate. Around iteration 36 we can see that a somewhat hexagonal pattern is shown however it is not stable as we can see that most of it fades away quickly after a few iterations.

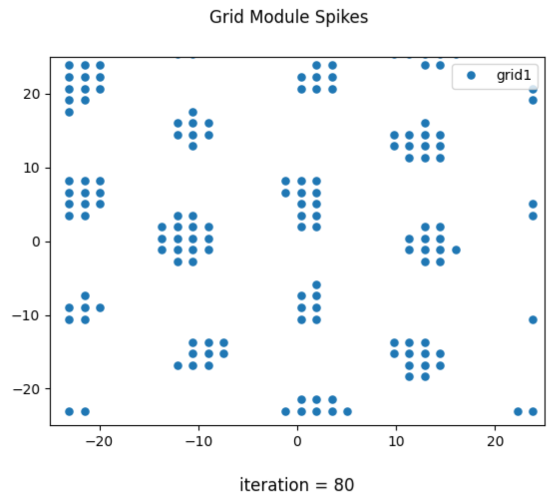

Figure 3.4: *Neural Spike Pattern after iteration* 80 *in the simulation, making a hexagonal shape*

Fortunately we can see Figure 3.4 that the hexagonal activity pattern has shown itself and it is stable from this point throughout the simulation. Also we have gathered information regarding the input current of neurons and their potential after making a hexagonal shape to get a better understanding of this pattern.

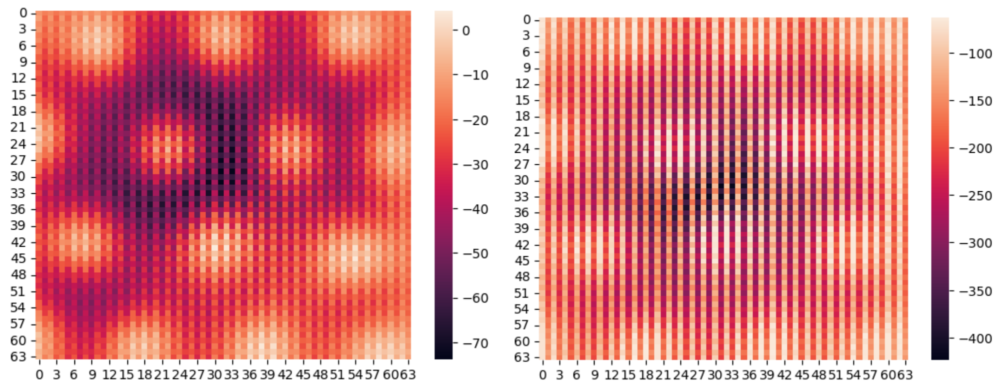

(a) *Heatmap of cells input current* **(b)** *Heatmap of grid cells potential*

Figure 3.5: *The hexagonal pattern of both their potential and their input current*

Now based on Figure 3.5, The combination of the hexagonal pattern of their potential and their input current will most likely result in a stable structure of hexagonal shape as intended.

In the next chapter, we are going to check the stability of the network and analysis its behavior while confronting a noisy input and whether it can keep the hexagonal shape after different levels of noise.

3.3 Scales & Orientation

Notably grid cells can be of different scales and also can have different orientations. Different sizes refer to the number of points of the hexagonal pattern and also their radius of neighbouring neurons firing toghether while different orientation can be formed of the same size but the hexagonal spike pattern can be oriented in a different angel from each other with having a shared center of activity whuch will help us in the next chapter for a more accurate spatial mapping and navigation. different scales can be achieved using different levels of inhibtion and the variance in the size of inhibtion rings.

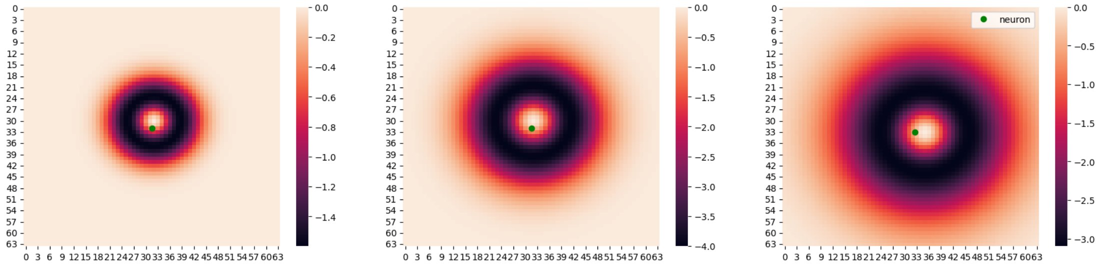

Figure 3.6: *different levels of inhibtion and sizes of the rings*

Figure 3.6 illustrates the different levels of inhibtion of each neuron. Small rings will most likely appear to have a more filled network with more active nodes or group of nodes which will then result in a more accurate movement mapping, also the bigger rings will result in a much more open mapping.

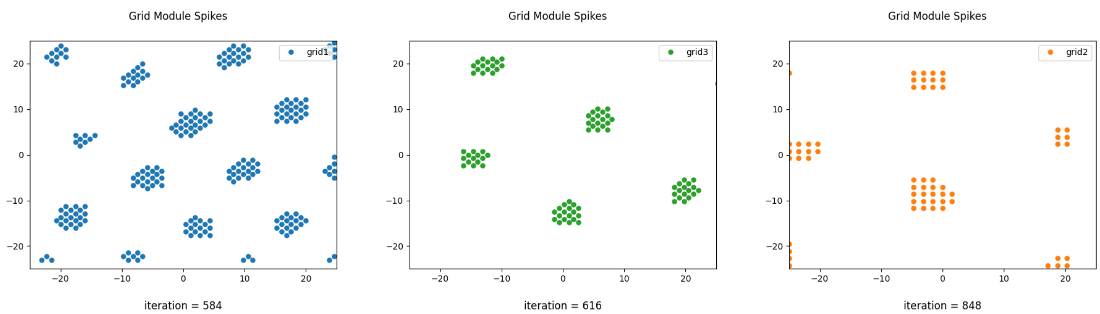

Figure 3.7: *three different scales of grid cell modules*

As we can see in Figure 3.7 we can get different scales of hexagonal spike pattern of grid modules by changing the ring of inhibtion.

Another way to achieve different scales is to use different scales of grid cells, for instance, we can have grids of scales $64 \times 64, 54 \times 54$ or 40×40.

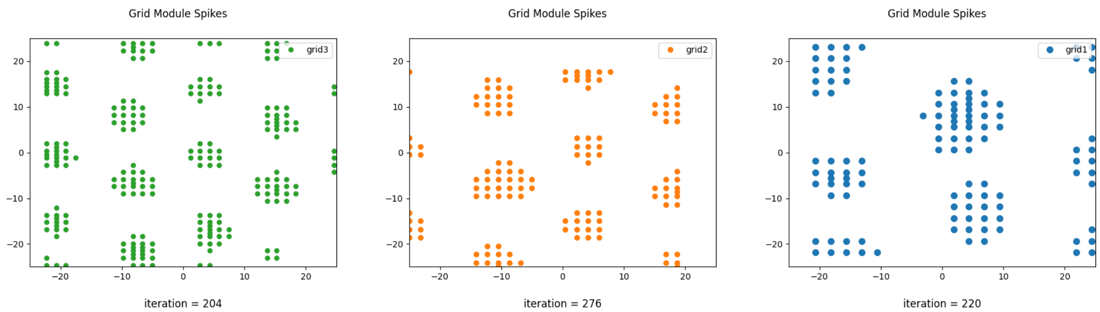

(a) $N = 64 \times 64$ **(b)** $N = 54 \times 54$ **(c)** $N = 40 \times 40$

Figure 3.8: *three different scales of grid cell modules using different number of neurons in each grid module*

Now in Figure 3.8, we can see here while the first type of scaling resulting in having more scales of movement, here we have different scales of positioning which both are highly crusial.

Now that we have developed a network of hexagonal shape, We are going to test its stability over different levels of input and noise and analysis its behavior in the next chapter.

4 Stability

In this chapter, we explore the robustness of neural activity and the hexagonal grid patterns in grid cells under conditions of noisy input and directional changes. We aim to understand how these cells maintain stable and consistent activity despite environmental fluctuations and navigational challenges, ensuring reliable spatial mapping and navigation.

4.1 Levels of input current

In Chapter 3, we saw the hexagonal spiking pattern of each grid cell module on fine-tuned parameters of input current. In this section we intend to use low and high level of voltage-based input current to see if the network can maintain its stability.

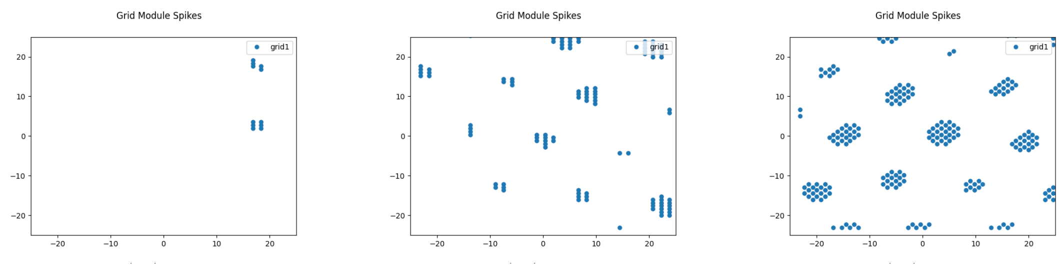

Figure 4.1: *grid cell module spiking pattern with* $I_{ext} = 15$ *and* $I_{vel} = 10$

Figure 4.1 shows that the network still has the hexagonal spiking pattern however, it might fade away in some iterations and not as strong as always but let's try to level up the I_{ext} without chaning the voltage-based input current to analysis its stability.

We can see some by Figure 4.2 improvement in the stability of the network simply by increasing the baseline input current although the voltage-based is relatively low.

note: In order to see the activity of the network throughout the simulation in short gifs you can check the link in the **supplementary materials** section of Chapter 6.

Now lets try to test the network stability on high level of input current.

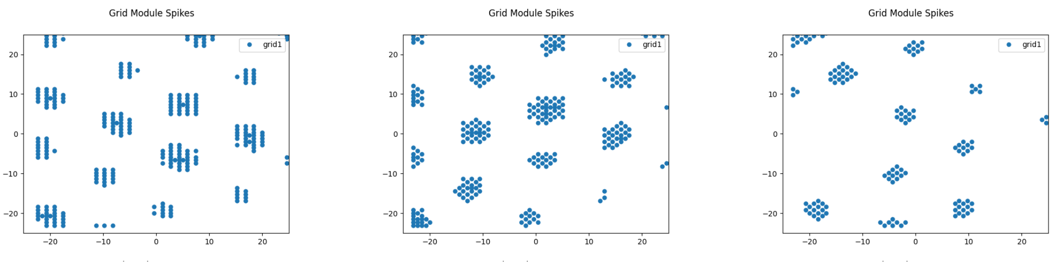

Figure 4.2: *grid cell module spiking pattern with* $I_{ext} = 30$ *and* $I_{vel} = 10$

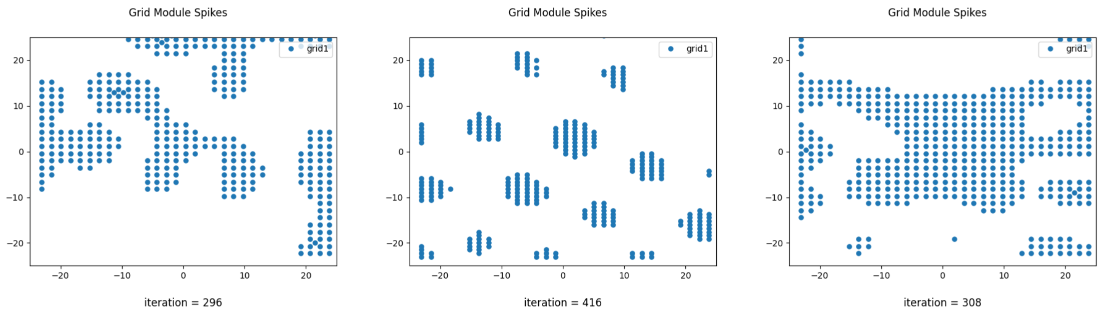

Figure 4.3: *grid cell module spiking pattern with* $I_{ext} = 20$ *and* $I_{vel} = 40$

Here we can see that due to high sensivity of the network to voltage-based input, with considerable constant input and low rate of inhibition the network falls out of balance and becomes unstable in some cases but it can also regain its hexagonal structure.

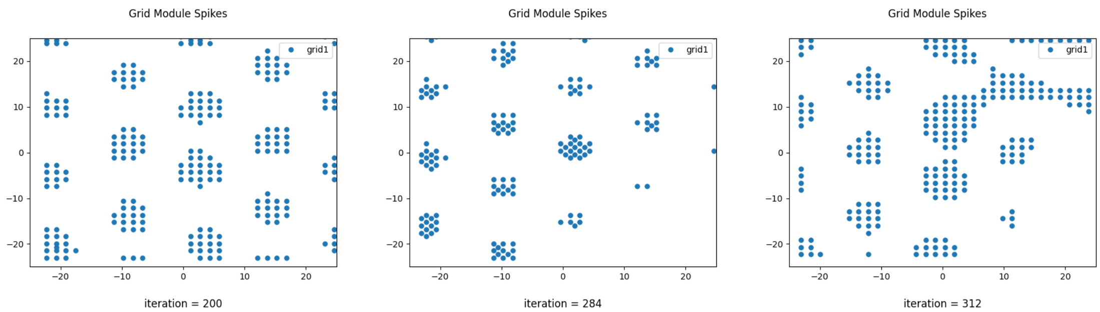

Figure 4.4: *grid cell module spiking pattern with* $I_{ext} = 5$ *and* $I_{vel} = 40$ *and* $1.5\times$ *lateral inhibition*

fortunately Figure 4.4 shows that we have also achieved a stable network while facing a high level of input current. (check out the supplementary materials for more details video).

4.2 Noisy input

Here we try to use the three noisy simulation movement we created in Chapter 2 to see whether the network can keep its stability with noisy input.

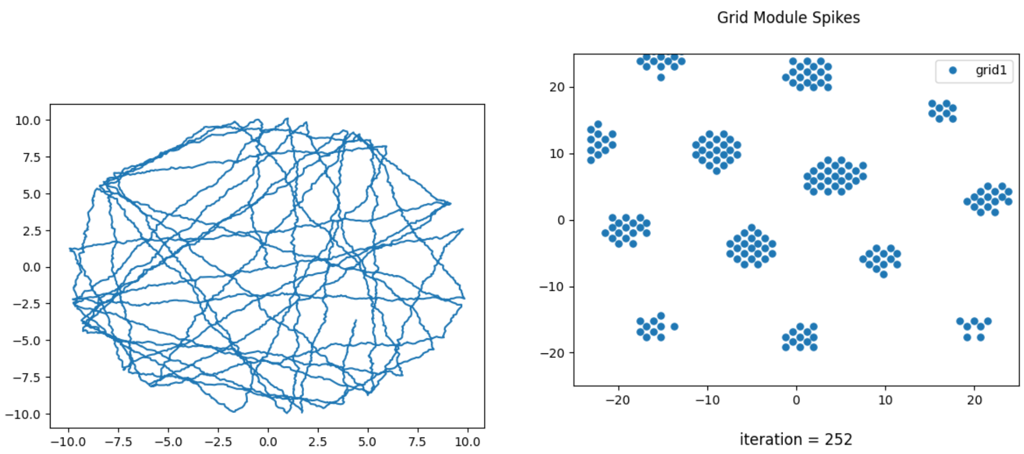

(a) *noisy navigation map* **(b)** *general activity pattern of grid cell module*

Figure 4.5: *grid cell module spiking pattern with average level of noisy input*

Here Figure 4.5 shows a stable structure throughout the simulation with an average level of noise in the input which our network passes the test fully. Now lets try a network of highly noisy input and see if network loses any stability.

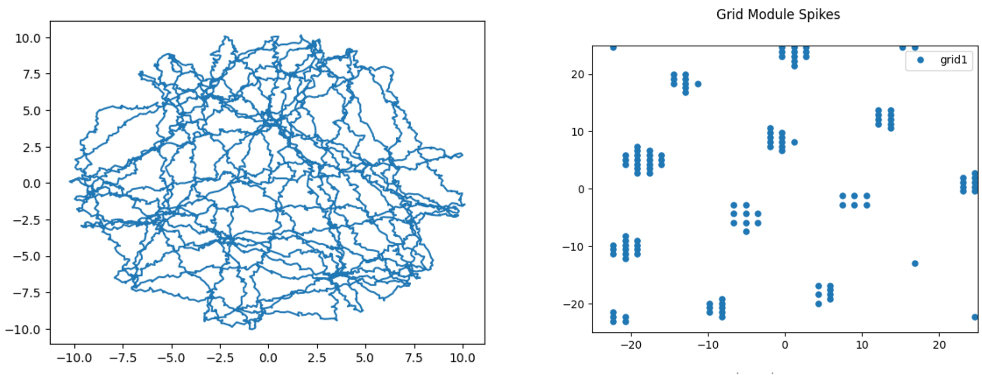

(a) *noisy navigation map* **(b)** *general activity pattern of grid cell module*

Figure 4.6: *grid cell module spiking pattern with high level of noisy input*

We can see in Figure 4.6 that the activity is still rather stable but due to lots of huge change of direction in few iterations the network might get into low levels of activity.

4.3 Change of direction

One last thing to check is the fact that how does the network behave while facing a **sudden change of direction**. As we saw previously from average noisy input small changes of direction does not affect the activity of the network however the sudden changes can be problematic.

Figure 4.7 shows different stages of activity throughout the sudden change of direction, as we can see we have the hexagonal structure before reaching the endpoint, in few iterations we can see considerable decrease in spiking activity however after **less**

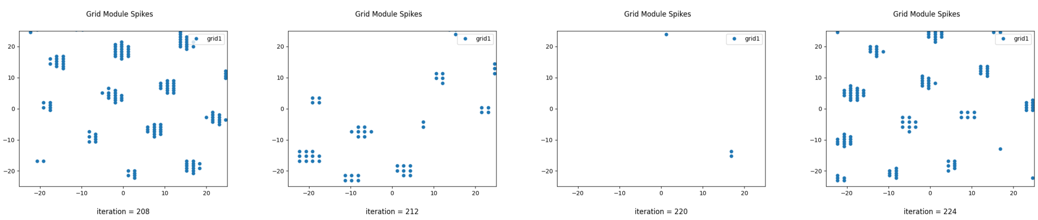

Figure 4.7: *different stages of neural activity when facing a sudden change of direction in the movement*

than 5 iterations we can see that the network has regained its stability and its hexagonal structure which is a good sign.

Now that we have stablished a stable structure of the network, in the next chapter we focus on movement and how we can use a combination of grid cell modules for accurate spatial mapping and navigation.

5 Spatial Mapping and Navigation

In this chapter, we examine how grid cell modules contribute to precise spatial mapping and navigation. We investigate the movement of these modules, their sensitivity to direction, and how multiple modules combine to form an accurate representation of space, facilitating effective navigation and spatial awareness.

5.1 sensitive directions

One of the most crusial and important behaviors we expect to see from grid cell modules is that with help of given dynamics and most importantly their **prefered direction**, they would be able to track movement and change their position based on real movement of the rat. In order to do this, neuron of each direction should be activated while the neuron is going in the direction of their e_{θ_i}.

Now Figure 5.1 shows that neurons are highly sensitive to their prefered direction and only neurons with their preferred direction matching the movement speed vector actually gets active and prepare the firing for the neighbouring neurons in their desired direction. But only sensing four main direction might not be enough for a full and accurate spatial mapping and navigation we have to see whether the network respond to the movement along different directions.

Fortunately we can tell from Figure 5.2 that not only they can detect movement particularly in their own direction but also they can work together to more accurately detect the direction of movement.

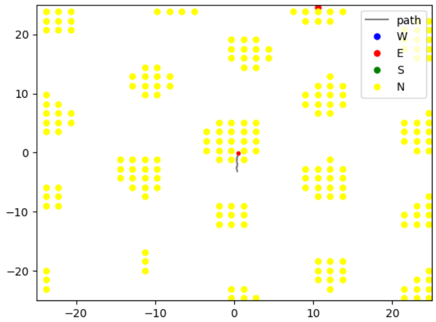

(a) *direction: North*

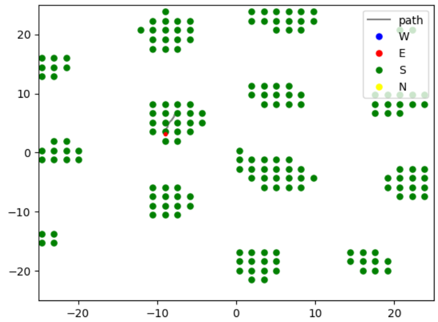

(b) *direction: South*

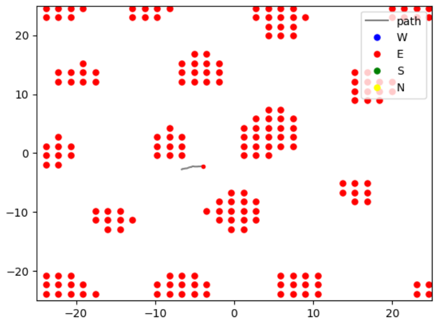

(c) *direction: East*

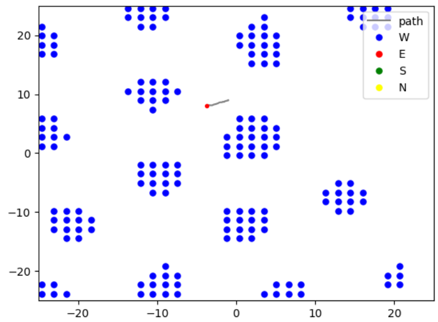

(d) *direction: West*

Figure 5.1: *activation of neurons based on their preferred direction sync with the direction of movement*

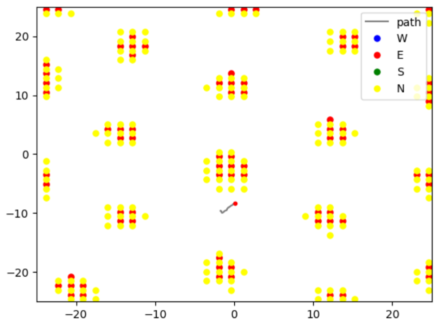

(a) *direction: North-East*

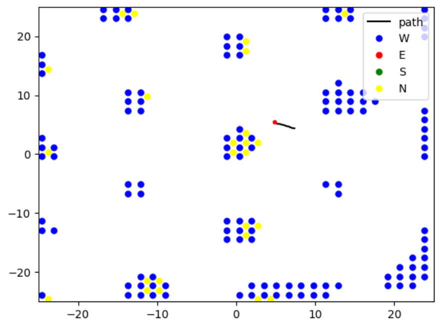

(b) *direction: North-West*

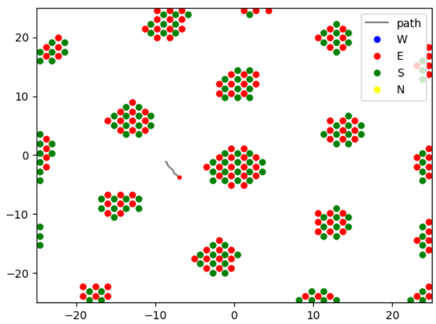

(c) *direction: South-East*

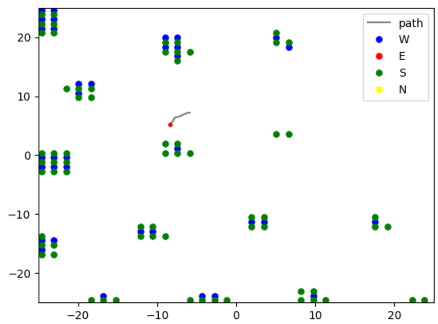

(d) *direction: South-West*

Figure 5.2: *activation of neurons based on their **combined** preferred direction sync with the direction of movement*

5.2 Grid Cell movement

Now that we know out network can detect the direction of movement we need to see whether it can actually move and navigate in their own space also known as *code space*. Meaning that by the movement of the rat in a certain direction, grid cells should also be able to move as a whole with a stable hexagonal pattern in the same direction.

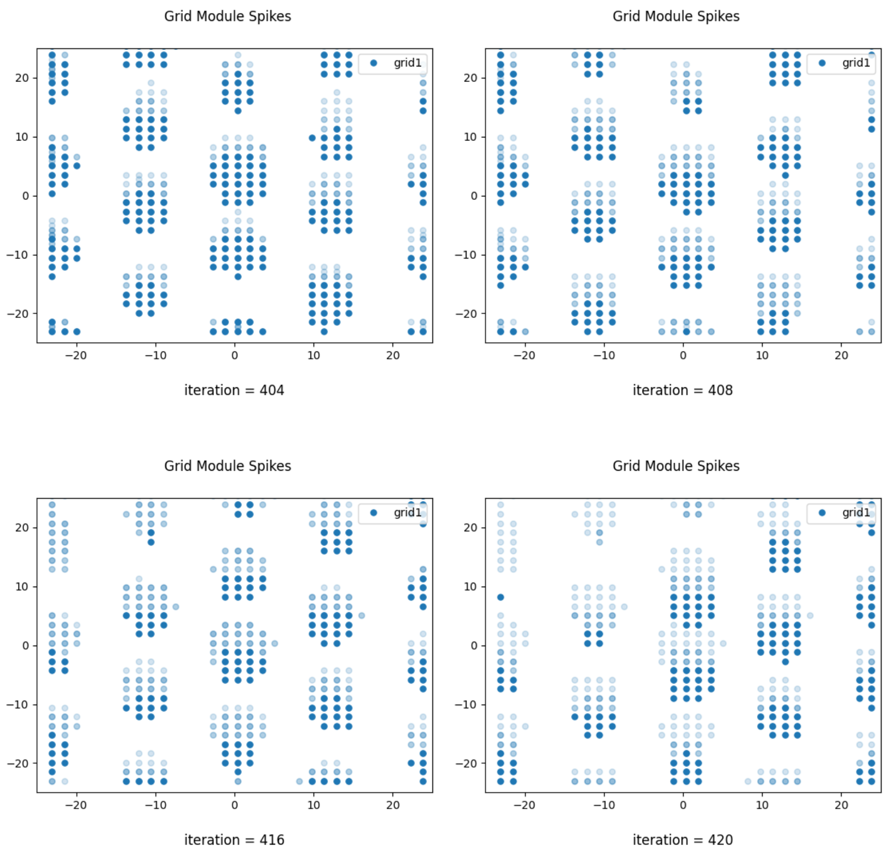

Figure 5.3: *raster plot of spiking pattern movement in accordance to rat's movement*

As we can see in Figure 5.3 the previous spikes are have lower opacity resulting in seeing the movement of neurons in the direction of movement. Also you can see that throughout different iterations a considerable movement of spiking pattern is visible.

Here Figure 5.4 clearly shows that not only it can have a smooth movement but also has great accuracy in changing the direction of movement and does a good job of tracking. Now that we have established the movement of activity in accordance to the rat's movement, we now need to use several modules for finding the accurate location instead of having several guesses.

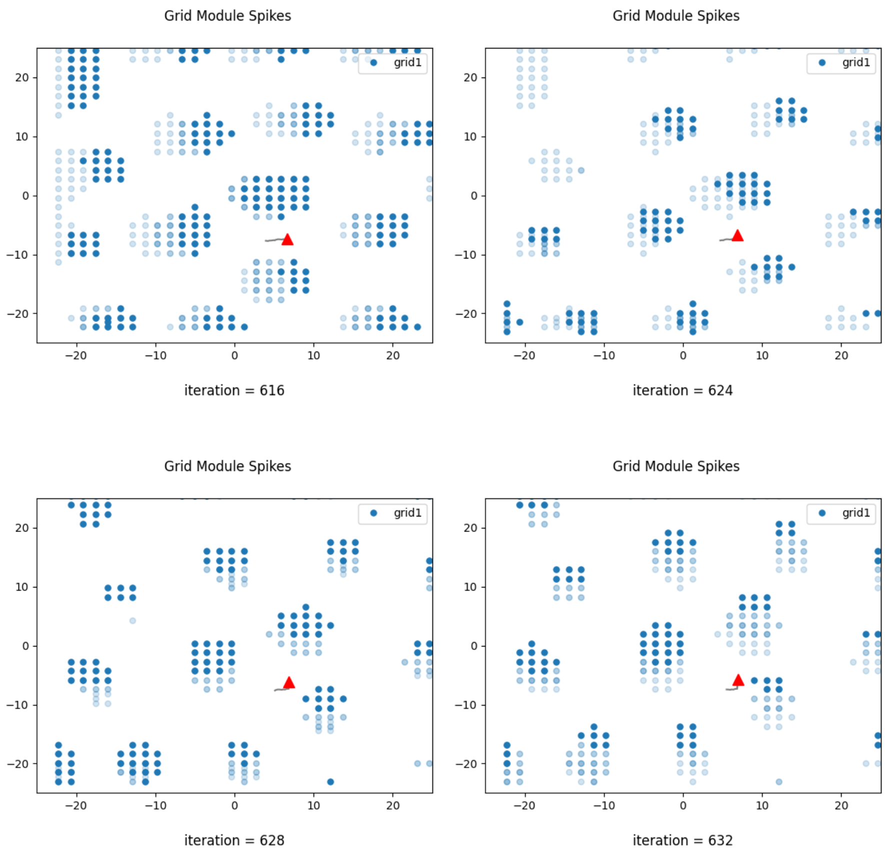

Figure 5.4: *raster plot of spiking pattern movement in accordance to rat's movement - **changing direction***

5.3 Multiple Grid Cells

This is the final work, as the combination of what we have developed throughout this project, with help of movement mechanism in this chapter and also generation of grid modules of different scales and oritentations we hope to achieve an accurate spatial mapping and navigation.

In this simulation we used three different grid cell modules in order to find unique location in the code space of the grid cells.

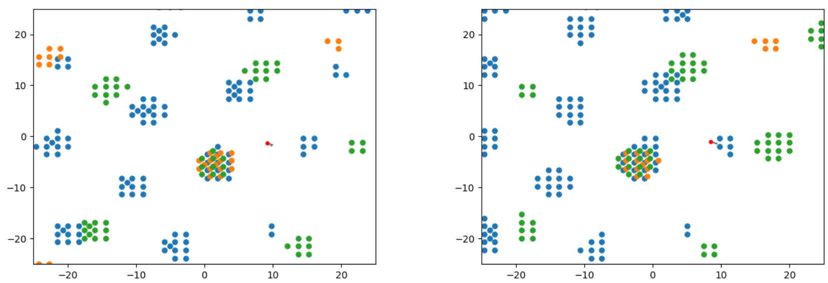

Figure 5.5: *accumulative raster plot of three different grid cell modules*

As Figure 5.5 shows we can see that all of these three modules center around one point which is the encoded location of the rat in the space of grid cells and also due to the movement of each grid cell seperately, they can keep the network intact and not only we can have an accurate location but also accurate movement.

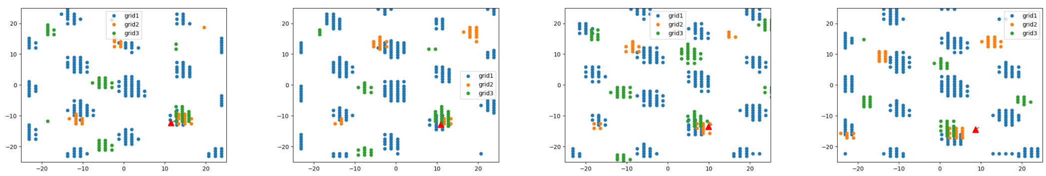

Figure 5.6: *accumulative raster plot of three different grid cell modules in a longer period*

We can also see in Figure 5.6 that this accurate mapping is stable and can be done once the grid pattern is created in each module.

important note. The location in which the combination of grid cell specify does not need to be the same location on the real world plane that the rat is at, the navigation starts with anchering a random location of the real world to a point in the grid cell module plane, and from then these two movement are a replica of each other only in different spaces and one can decode it using a simple transformation.

6

Conclusion & Future Work

6.1 Conclusion

In this project, we developed a comprehensive computational model to understand the function of grid cells in the L6 layer of the neocortex. Through simulating rat movement, we generated realistic input data to observe grid cell activity. We proposed a spiking model using the LIF framework within a continuous-attractor-network to replicate grid cell dynamics. We analyzed the stability of neural activity and hexagonal patterns under varying conditions, and explored how multiple grid cell modules interact to create accurate spatial mapping and navigation. This integrated approach provides valuable insights into the mechanisms of spatial cognition and the role of grid cells in the neocortex.

6.2 Future Work

In this project, the orientations of grid cells were initialized randomly. Future work should focus on developing a method to achieve more controllable orientations, potentially by specifying the degree of orientation to generate different grid module patterns systematically. Additionally, the center of activity in our simulations was randomly assigned. To enhance the model's reliability for navigation, we need to establish a stable and focused center of activity consistently. Addressing these aspects will improve the precision and applicability of our grid cell model for spatial mapping and navigation studies.

6.3 Supplementary materials

Due to the importance of movement in this project and also the 2D nature of the grid modules we have created a few *.gif* files which gives a better understanding of the movement and the final activity of the grid cells. You can access the supplementary materials here.

This page intentionally left blank.

UNIVERITY OF TEHRAN

COMPUTATIONAL MODEL OF L6 LAYER,
CORTICAL GRID CELLS

ARASH NIKZAD
Student No. 610301195

TEHRAN, JULY 2024